ANNEX A3

CO_2 Storage Liabilities in the North Sea –

An Assessment of Risks and Financial Consequences

Fault
Study

Simon Mathias
Durham University

Status	**FINAL Draft**
Date	**16th May 2012**
Issued by	**Stephen Jewell**

Annex A3 - Contents

1.0 Introduction - Leakage through faults

As discussed in the previous section on caprocks, the primary concern of leakage through caprocks is the migration of CO_2 through fault zones and leaking wells. In this section, we discuss the specific issue of CO_2 leakage through fault zones.

But before starting, it is worth to recall the geological section from the Southern North Sea Basin (SNSB) shown in Fig. 1a of the previous section. Note that most faults are at the Permian level and do not extend upwards beyond the Zechstein. In fact there is little faulting in the Jurassic and younger sections of the SNSB. This is important as it implies that fault pathways do not extend upwards from Rotliegendes to surface. In addition the transmissivity of faults through sealing sections are likely to be very low.

Although the tectonics and structural evolution are different in the Central and Northern North Sea Basins, few of the faults at Jurassic and older levels extend upwards through the Cretaceous and Tertiary sections, and there is little large scale faulting in the shallow formations (see Fig. 11). The faulting is largely in pre- and syn-rift stratigraphy in the North Sea. Note that the 100s of metres of overlying quaternary deposits are likely to contain many additional low permeability layers.

Nevertheless, it is important to develop a good understanding of how leakage of CO_2 through faults may progress. In this section, key features of technical basis concerning leakage through faults are presented and discussed. These mostly relate to fault permeability. Following from this, CO_2 leakage rates through faults and fractures are reviewed from natural analogue studies in the literature. A state of the art review is then presented concerning numerical simulation of CO_2 leakage through faults. Finally the work is summarised and concluded with semi-quantitative statements concerning duration, nature and magnitude of likely leakage rates expected from future CO_2 storage projects.

2.0 Fault zone structure and permeability

Faults come about where hard rocks under pressure have failed via shear or tension. Such features are seen as discontinuities in the laterally adjacent lithologies (Fig. 1) and can be identified in deep formations as discontinuities in seismic reflectors (Fig. 2). They can also be seen on some wireline logs and observed in core. Fault zones typically consist of a damage zone and fault core and may contain a single or multiple fault core sequences (Fig. 3). Fault zone structure depends on the depth of formation, lithology, tectonic environment (extensional, compressional etc.), throw (magnitude of displacement) and fluid flow (Faulkner et al., 2010). For instance, faults in low porosity rocks generally have a fine-grained fault core surrounded by a fracture dominated damage zone. Conversely, in coarser grained high porosity rocks, the damage zone tends to be comprised of low porosity deformation bands (sometimes referred to as granulation seams) whilst the core maintains a higher permeability slip surface.

2.1 Permeability of faults

A primary factor concerning leakage of fluid through faults is the so-called permeability. Fluid flow in porous media is generally controlled by Darcy's law, which stipulates that flow per unit area, q [m / s], is found from $q = - k J / \mu$ where k [m^2] is permeability, (Bear, 1972) J [Pa / m] is pressure

gradient and μ [Pa s] is fluid viscosity. Typically, permeability is measured in milli-Darcies (mD) where 1 mD = 10^{-15} m^2. A good reservoir rock typically has a permeability of 50 to 1000 mD for geological storage of CO_2. A good seal might be expected to have a permeability < 10^{-4} mD.

Estimating the permeability of faults is not straightforward. The standard procedure to estimate permeability of a given geological formation is to emplace a rock core (typically around 1 to 10 cm in scale) within a permeameter and to measure the flow rate of fluid that results from a given imposed pressure gradient. Such an approach is reasonable if the physical structures controlling the flow fluid are much smaller than the scale of the rock-core being studied. However, for faults this is not possible as fault properties vary on multiple scales both across and along the fault.

For instance, Fig. 4 shows a schematic of the expected permeability distribution across the core and two flanking damage zones for a low porosity rock. The permeability of the individual fractures are high whereas the permeability of the core is expected to be low (note that exactly the opposite occurs in coarse grained high porosity rocks containing granulation seams). It can be shown mathematically (Bear, 1972) that a good estimate of the bulk permeability across the fault can be obtained from a weighted harmonic mean of the individual permeability components (Manzocchi et al., 1999). Note that across the fault, the low permeability components act as bottleneck restrictions to flow. But such a value will not be appropriate for describing permeability of the fault along the fault. This gives rise to anisotropy in permeability. Generally it is perceived that faults are more permeable along the fault than across the fault (Bense and Person, 2006).

2.2 Behaviour of faults during reactivation

It is widely understood that CO_2 injection into a potential reservoir should avoid leading to excessive pressure buildup such that the mechanical failure of the cap-rock may occur (Mathias et al., 2009). Two modes of failure are generally considered. Firstly, one should be concerned about the generation of new fractures within the cap-rock due to tensile failure. But secondly, care should be taken to avoid shear-failure, which is most likely to occur in critically oriented pre-existing fault zones (Streit and Hillis, 2004). In the context of leakage of CO_2 through faults, reactivation of faults should certainly be avoided. Streit and Hillis (2004) also discussed that for a pressure depleted field, there is the possibility, depending on the rock matrix characteristics of the reservoir (e.g. grain on grain), for production related geomechanical effects to have caused microfracturing in the rock grains. Thus, if such fields are re-pressured with CO_2 injection, then the faults in the field may fail at pressures lower than the original pre-production pressures.

There is growing bulk of evidence suggesting that fault permeability is greatly enhanced as the stresses approach critical state (Faulkner et al., 2010). Transient increases in up-fault permeability during periodic reactivation is perceived to have been partially responsible for several leaked fault-bounded hydrocarbon traps in the Northern North Sea (Wiprut and Zoback, 2002). Measurements of fault permeability (probably using seismic methods) in the Pathfinder well on Eugene Island, Gulf of Mexico, were found to originally to be around 1 mD but increased to as high as 1000 mD as fluid pressures increased towards the minimum principal stress (Losh and Haney, 2006).

2.3 Fault transmissibility multipliers associated with cross fault permeability

Conventional methods for numerical simulation of oil and gas reservoir operations involve discretising the physical domain on to a relatively coarse model grid (typically of the order of 100

m in plan). Fault zone thicknesses are highly variable but generally < 10 m thickness. Rather than gridding out the smaller scale features, modellers often impose an effective transmissibility multiplier on those grid-cells lying either side of a given fault. Much work has been undertaken to develop suitable algorithms for assessing transmissibility multipliers from more obtainable data (Manzocchi et al., 2010).

Myers et al. (2007) defines transmissibility as "the volume weighted average permeability of two connected cells or nodes in a flow simulation model". It has units of permeability × length. Faults affect the transmissibility by altering connections and interposing fault materials between cross-fault juxtaposed cells. A typical approach for calculating fault transmissibility multipliers begins with identification of cross-fault sand-on-sand connections in the geological model. A fault zone thickness and permeability are then determined from the throw of the fault and the predicted composition of the fault rock at each connection. Fig. 5 shows examples of some relationships that have been adopted in the past. The reader is directed to Myers et al. (2007) and (Manzocchi et al., 1999; 2010) for more detail. An important consideration is that these methods are only suitable for estimating cross-fault permeability of faults. The motivation here is linked more to the role of faults in reservoir compartmentalisation, discussed in more detail later in the report.

2.4 Air permeability measurement of fault zones at Yucca Mountain.

A more direct method for assessing in situ permeability of fault zones is to perform and interpret some form of in situ pressure interference test. Many different approaches have been used to attempt to quantify the significance of faults as permeable pathways at the (previously) proposed US high-level radioactive waste disposal site in Yucca Mountain, Nevada. Lecain (1998) describes an air injection study of faulted volcanic tuffs. Essentially this involves installing a packer over an interval within a vertical borehole where a fault zone intersects. Air is then forced into the interval at a monitored rate. The pressure buildup is then recorded and inverted, using a mathematical flow model, to infer the bulk permeability of the horizon. Lecain (1998) observed a range of fault-zone permeabilities from 1100 to 41,000 mD.

2.5 Estimation of along fault permeability using seismic methods

Implicit estimations of along fault permeability (AFP) can also be obtained from observing the migration of seismic events using seismometer arrays. (Note: Seismic events from earthquake data should not be confused with seismic 'reflection' data used to obtain profiles of the cross-section of sedimentary basins.) Assuming seismic events are caused by pore-pressure induced shear-failure of faults, seismic event migration data can be translated to pore-pressure wave migration data along the fault zone of concern. This in turn can be used to estimate hydraulic diffusivity (= mobility / compressibility). Given a set of values of porosity, compressibility and viscosity, the hydraulic diffusivity can be used to obtain an estimate of permeability. Talwani et al. (2007) applied this method to estimate AFP at a range of different sites across the world, concluding that along fault permeability should generally range between 0.5 and 500 mD. However, several studies apparently overlooked by Talwani et al. (2007) include that of Miller et al. (2004) who observed AFP in an Northern-Apennine-carbonate sequence to be 40,000 mD and Noir et al. (1997) who inferred an AFP, in the Gulf of Aden, of 10^7 mD.

One issue of concern is that these excessively large measured permeabilities from seismic events may be due to permeability enhancement, due to pore-pressure increase, associated with the seismic events. This has important implications for planning for CO_2 leakage because similar faults

may remain as sealing faults provided they are not significantly perturbed by ambient or anthropogenic local stress changes. Furthermore, critical stress associated permeability changes may be highly episodic (Wilkinson and Naruk, 2007) and therefore, the duration of possible corresponding leak events may be very small. More work is clearly needed to understand this feature further. There are areas on the NW shelf of Australia, where the petroleum exploration concept is to examine fault orientations, as those parallel to the compression collision direction with Timor did not result in hydrocarbon leakage, whereas those perpendicular resulted in fault failure and leakage of trapped hydrocarbons (O'Brien and Woods, 1995).

3.0 Faults as barriers and conduits

When considering the risk of CO_2 leakage through faults, it is important to bear in mind, that faults often form impermeable barriers to the migration of hydrocarbons over geological timescales (Bretan et al., 2011). Note that the main objective of the aforementioned fault transmissibility multipliers is to represent how low (as opposed to high) the cross fault permeability (CFP) is at a given reservoir fault boundary.

There are primarily two ways in which faults are thought to seal and compartmentalise reservoirs (Gluyas and Swarbrick, 2004). The first is known as a juxtaposition seal whereby a reservoir formation is displaced such that it is sealed by a newly adjacent low-permeability layer (salt, shale, mudstone etc.). The second mode is due to smearing, whereby sealing rocks (shales and/or clays) are smeared across the fault boundary to form an impermeable vertical bounding layer (Fig. 6) (van der Zee and Urai, 2005). Compartmentalisation due to fault sealing often leads to underestimates in gas yields; for example in the Southern North Sea, Rotliegend Sandstones (van Hulten, 2010). Such an affect has also been highlighted as an issue for the CO_2 storage capacity in the recently completed, ETI (Energy Technology Institute) funded UK Storage Appraisal Project (UKSAP) (Gammer et al., 2011).

On the other hand, faults can also form preferential flow paths for vertical fluid flow. Evidence of faults acting as conduits includes extensive mineralisation patterns (e.g. see Fig. 7), leakage of contaminated groundwater along faults, preferential oil migration via faults, geothermal anomalies and expulsion of overpressure fluids along faults (Bense and Person, 2006).

4.0 Natural analogues for CO_2 leakage through faults

Arguably the best way to assess potential rates of leakage from faults which are leaking, is to investigate existing sites where CO_2 has been or is currently leaking. Lewicki et al. (2007) compiled observations from 13 natural and 8 anthropogenic CO_2 leakage events.

The sources of CO_2 in natural accumulations were found to be most commonly thermal decomposition of carbonate-rich sedimentary rocks and/or degassing of magma bodies at depth. CO_2 from these sources was often found to accumulate in permeable formations (e.g. sandstones and fracture limestones) under low permeability cap rocks (e.g. shale and siltstone).

In the case of the natural CO_2 leaks, once the CO_2 moves from the storage reservoir, faults were often found to be the primary leakage pathway (8 out of the 13 natural leakage events studied). Those events where attempts were made to quantify the rate of CO_2 leakage are summarised in Table 1. Lewicki et al. (2007) comments that it is not clear whether the associated high permeability pathways were pre-existing or created/enhanced due to seismic event activity

associated with the fluid migration. Note that in all the anthropogenic events, the wells were found to be the primary leakage pathways.

Some of the natural CO_2 leakage events were correlated with specific triggering events, such as seismic event activity or magmatic fluid injection, while other events were not correlated to such events. However, the lack of correlation in the latter cases may have been due to the absence of data collection at the time of the leakage event.

The nature of the CO_2 release at the surface was quite varied including diffuse gas emissions over large land areas, focused vent emissions, eruptive emissions and degassing through surface water bodies and spring discharges.

Monitoring strategies applied included measurements of soil CO_2 flux using accumulation chamber or eddy covariance methods and soil, atmospheric, or vent gas CO_2 concentration using gas analyser or chromatography techniques.

The reader is strongly recommended to look at the supplementary information provided with Lewicki et al. (2007) for further detail.

The data from Lewicki et al. (2007) is summarised along with additional data concerning leakage through faults and permeable zones given by Streit and Watson (2004), Pearce et al. (2002) and Chiodini et al. (1999) in Table 2. Because the associated areas are not known for all the sites, these are displayed in t / yr / m^2. The term permeable zone is used here to describe permeable silt and sand lenses or subseismic fault-fracture networks (Streit and Watson, 2004).

5.0 Numerical simulation of CO_2 leakage through faults

Much work has focused on mathematical and numerical simulation of CO_2 injection and storage in geological reservoirs. However, this has mostly focused on pressure buildup (Mathias et al., 2011), plume geometry development and residual trapping (Pruess and Nordbotten, 2011). Nevertheless, a number of modelling studies have also looked at the topic of leakage of CO_2 through faults.

5.1 A simple equation

Arguably, the most simple approach is that presented by Humez et al. (2012), who simply state that the rate of leakage, M_{leak} [kg/s], of CO_2 through a fault of cross-sectional area, A [m^2], can be estimated from

$$M_{leak} = - \rho_{CO2} A k k_r (J - \rho_{CO2} g \cos \theta) / \mu_{CO2}$$

where ρ_{CO2} [kg/m^3] is the density of CO_2, k [m^2] is permeability, k_r [-] is a permeability reduction factor due to the presence of residually trapped brine, J [Pa / m] is the pressure gradient along the fault, g [m/s^2] is gravitational acceleration, θ is the angle of orientation of fault to the vertical axis and μ_{CO2} [Pa s] is the viscosity of CO_2. Note that if the system is under hydrostatic conditions (in terms of water), $J = \rho_w g \cos \theta$ where ρ_w [kg/m^3] is the density of the formation water. Values of k_r can be estimated from the end-point relative permeability data presented by Bennion and Bachu (2009) and ranges from 0.0000828 (an anhydrite) to 0.5446 (a sandstone). More recently, Tueckmantel et al. (2012) measured the relative permeability of a brine CO_2 mixture in cataclastic fault rocks in porous sandstone from the 90-Fathom fault (northeast England). Unfortunately, the

data are only shown on a log-scale so the end-point is not easily ascertained. However, from a visual inspection of the graph, it looks to be very close to 1.0.

5.2 Effect of leak-off into overlying layers

Chang et al. (2008) developed a similar fault model to above but also accounted for leak-off into overlying permeable formations and permeability variation along the fault. The latter is an important point as a fault is unlikely to be conductive continuously from depth to the shallow subsurface. The permeability in the direction of the fault throw can be particularly small in regions where sufficient shale or clay is entrained within the fault. Chang et al. (2008) set the top of their faults as hydrostatic and the bottom as over pressured. The value of over pressure is assumed to be proportional to an assumed height of the CO_2 column in the storage reservoir.

The article finds their simplified approach to compare favourably to a set of more sophisticated 2D simulations performed using the commercial simulator, CMG GEM. For one scenario discussed in detail, where fault permeability was assumed to be 1000 mD, it is found that the storage formation leaks CO_2 at a rate of 0.26 kg/s/m^2. But, because of leakage into overlying formations, the surface release rate is just 0.07 kg/s/m^2. For a more shallow scenario, the leakoff was much less, such that whilst the storage loss was 0.12 kg/s/m^2 the surface release was 0.08 kg/s/m^2.

5.3 Effect of fault orientation

Chang and Bryant (2009) present more realistic simulations whereby the fault leakage and the storage formation are fully coupled. Here the objective is to study how the injection plume is affected by the presence of the fault. They study three different cases. (1) a declined (inclined in the opposite direction of the injected CO_2) sealing fault, (2) a conductive declined fault and (3) a conductive inclined (inclined in the direction of the injected CO_2) fault. For case 1, the CO_2 accumulates at the side of the sealing fault. For case 2, once the CO_2 plume makes contact with the fault, the CO_2 starts to rise up the fault a little and then continues to migrate across the fault into the reservoir unit on the other site. For case 3, the CO_2 simply migrates up the fault on contact.

From the results in case 2, the authors suggest that the orientation may be a major factor on whether CO_2 can migrate up to the surface. However, this finding is largely due to Chang and Bryant's (2009) assumption that the fault permeability is isotropic. As discussed earlier in the report, fault permeability is more likely to be anisotropic and larger along the fault than across. Should Chang and Bryant (2009) have invoked a more realistic anisotropy for their case 2, it is expected that the CO_2 would have continued to migrate up the fault as with their case 3.

5.4 Effect of fault connectivity

Lee et al. (2010) were interested to investigate the role of fault connectivity on CO_2 leakage. They set up a numerical simulation whereby CO_2 was injected into a sandstone reservoir at 1000 m depth. The CO_2 was then allowed to leak into a sequence of five overlying fault zones inter-connected by additional sandstone sequences (see Fig. 8). The permeabilities assumed for the sandstone and fault zones were 50 and 1000 mD, respectively. Results from the simulation found that, despite a substantial leak from the storage reservoir, CO_2 rose by just 500 m after 1000 years and only an additional 40 m after 5000 years, such that leaked CO_2 never came within 460 m of the ground surface during the 5000 year period studied.

5.5 On the role of thermodynamics

All the simulations described above have assumed isothermal conditions and single or two-phase flow. Interesting transient effects are observed when one considers non-isothermal conditions and the full three-phase problem. Below 800 m depth, CO_2 is expected to be supercritical and present as a single phase. Therefore, when dealing with CO_2 and brine mixtures at depth, it is appropriate to assume a two-phase system. However, above 800 m depth, CO_2 can be concurrently present as both a gas and liquid phase. Hence, with the brine as well, a three phase system can occur. The presence of three fluid phases leads to significantly increased phase interference at the pore-scale and consequential reductions in relative permeability.

Pruess (2005) used the non-isothermal three-phase simulator, TOUGH2, to investigate the role of geothermal gradients, three-phase flow and thermodynamics on leakage of CO_2 though faults. Specifically, he considered supercritical CO_2 rising up the corner of a 2D fault plane. As the CO_2 rose, the CO_2 expanded, due to the reduced pressure, which in turn led to Joule-Thomson cooling. This reduction in temperature brought CO_2 out of the supercritical regime and both a gas and liquid phase developed. The resulting three-phase system (brine along with gaseous and liquid CO_2) gave rise to a reduction in relative permeability and a consequential reduction in CO_2 migration rate. However, once the migration rate was reduced, CO_2 expanded at a slower rate, and the surrounding geothermal heat allowed the CO_2 to warm up again such that supercritical conditions and the associated more mobile two-phase system reappeared. CO_2 then continued to migrate upwards and expand and the whole process repeated in a periodic sequence.

Since then, Pruess (2011) coupled his fault model to an injection reservoir model to provide a more realistic base-of-fault leakage flux (see Fig. 9). The result at surface was the periodically increasing and decreasing CO_2 leakage rate shown in Fig. 10. For this scenario it took 187 years for the plume to arrive at the fault and then an additional 10 years for the CO_2 to arrive at surface (about 1000 m). The fault was assumed to have a permeability of 500 mD and the mean pseudo-steady-state leakage rate was around 4×10^{-4} kg/s/m^2 (quite a lot lower than those rates predicted by Chang and Bryant, 2008).

Surface leakage results from the numerical studies of Chang et al. (2008) and Pruess (2011) are compared with those from the natural analogue studies presented previously in Table 2. The Pruess (2011) result is consistent with Latera and Matraderecske events (the largest natural analogue rates reviewed) reported by Pearce et al. (2004). The Chang and Bryant (2008) estimates are three orders of magnitude larger. Further work is certainly needed to better understand the significance of this discrepancy.

All the above studies explicitly assume that the CO_2 plume of concern encounters a fault through which to leak. But the risk of leakage of CO_2 through faults is strongly dependent on the probability of the plume encountering a conductive fault network that leads to a leak at surface (Zhang et al. 2010).

It must however be recognised that if a fault is 'leaking', and if reservoir pressure is increased due to CO_2 injection and storage, the formation fluids will enter the permeable fault zone and may be detectable as a potential leak point well before any CO_2 fluid reaches that zone.

6.0 Summary and conclusions

In the context of the North Sea, it is important to consider that most significant fault zones do not extend through the quaternary deposits (e.g. Eratt et al., 2011). Fault zone structures are highly variable. Typically these are comprised of a core surrounded by a damage zone. In high permeability rocks, the damage zone represents lower permeability, due to compression of voids (Faulkner et al., 2010). For low permeability rocks, the damage zone can be highly fractured and represent significant permeability. The core in faults is often expected to be of low permeability due to the smearing of low permeability rock across the fault plane. Shale gouge ratio (SGR) represents a quantitative measure of this effect (Manazocchi et al., 2010).

The presence of planar fault cores surrounded by damage zones gives rise to significant permeability anisotropy (Bense et al., 2006). Where damage zones represent high permeability regions, flow along the fault will follow high permeability pathways. In contrast, flow across a fault zone is more likely to be blocked by the low permeability core, leading to low effective cross-fault permeabilities. Note that high SGR is generally considered to correspond to low cross-fault permeability.

Fault zone permeabilities are often represented in reservoir simulators using fault transmissibility multipliers (FTM) (Manazocchi et al., 2010). These allow faults to be represented in 3D coarse grid models as a 2D line feature. However, most of our understanding concerning FTM has been derived from a desire to quantify the sealing potential of faults. Such information therefore predominately relates to cross fault permeability. But CO_2 leakage through along faults will be controlled by along fault permeability (AFP). Note that many gas reservoirs are compartmentalised by faults. Fault sealing comes about due to juxtaposition of reservoir rocks with sealing rocks (e.g. shales and evaporites) and smearing of clay and shale in fault zones from surrounding formation units (Bretan et al., 2011).

Information concerning AFP is scarce. The main issue concerns our ability to measure AFP. Permeability of low permeability rocks can be observed from permeameter testing of rock cores. AFP on the other hand can only be measured in situ. Air permeability testing of faulted volcanic rocks at Yucca mountain yielded values ranging from 1100 to 41,000 mD (LeCain, 1998) (for reference, a good reservoir rock typically has a permeability > 50 mD). Implicit measurement based on migration of seismic events has led to observation of AFPs as high as 10^7 mD (Noir et al., 1997). But the latter could be more a reflection of the permeability enhancement that occurs when faults approach a pressure induced critical state (i.e., just before reactivation) (Losh and Haney, 2006). The truth is that there is a large degree of uncertainty associated with along fault permeabilties.

A range of natural analogue studies where CO_2 has been observed from faults, fractures and high permeability zones are discussed in the literature (Pearce et al., 2002; Hillis and Watson, 2003; Lewicki et al., 2007). Relevant leakage rates are summarised in Table 2. Most documented leakage rates are less than 1 t / yr / m^2 although the highest rate recorded was at Latera in Tuscany at 40 t / yr /m^2 (Pearce et al., 2002).

A number of numerical simulation studies have been undertaken to look at leakage of CO_2 through fault systems. However, these have mostly used simple conceptual models involving single faults intersecting a storage reservoir unit. Simulated leakage rates are only reported from two studies

(Chang et al., 2008; Pruess, 2011) and are at the high end of rates observed from the natural analogues (Table 2). Thermodynamic effects can play an important role on the transient response of leakage rates (Pruess, 2011) although these are unlikely to significantly affect the long-term rate. A major issue with leakage rates from numerical simulations are their high dependence on the permeability distribution assumed for the fault zone.

6.1 Critical controls on Leakage

Critical controls on leakage of CO_2 through faults include along fault permeability, CO_2 injection induced pressures leading to fault reactivation and fault pathways leading to a connected pathway of permeability to the surface.

6.2 Potential leakage rates

Providing the CO_2 plume is not intercepted by faults, leakage of CO_2 through faults will be zero. But note that, as with intact caprock, faults also have a capillary sealing potential (see Underschultz, 2007). Providing the capillary seal is maintained, the CO_2 leakage rate through the fault should be zero. If the CO_2 plume intersects with a connected fault zone and the capillary seal is broken, CO_2 leakage through the fault zone will be dependent on the along fault permeability. Natural analogue studies suggest that leakage rates could be as high as 40 t / year / m^2. The limited number of modelling studies available from the literature suggest even higher rates. However, there is considerable uncertainty attached do model predictions due to poor knowledge concerning along fault permeability.

6.3 Potential leakage duration

For all of the outcomes listed above, leakage will ultimately be driven by permeability, buoyancy drive and pressure gradient. For closed reservoirs, pressure is expected to decline with time. Fault permeability and pressure gradient are both expected to reduce with reducing pressure. Consequently, CO_2 leakage rates can be expected to reduce with time. However, for open reservoirs, aquifer drive may lead to sustained reservoir pressures despite leakage. Consequently leakage may ultimately continue until the CO_2 reservoir is emptied of buoyant fluid.

6.4 Variation of risk through storage life cycle

Leakage of CO_2 through fault zones can only occur once enough time has passed for the CO_2 to intersect a fault zone. The CO_2 plume will continue long after injection has ceased due to the Buoyancy drive. The probability of the plume intersecting a fault zone therefore becomes greater with increasing time. However, the significance of the fault zone as a leakage conduit is driven by the reservoir pressure because faults are expected to be significantly more permeable at critical state (i.e. close to reactivation). The critical time for pressure is during injection. The risk of fault reactivation dramatically decreases once CO_2 injection is stopped. Following CO_2 injection the probability of fault reactivation will mostly be driven by externally induced seismic events or nearby reservoir engineering activity (e.g. oil and gas or new CO_2 storage projects).

7.0 References

Bear (1972) Dynamics of Fluids in Porous Media, Dover Publications Inc.

Bennion D. B., and S. Bachu (2008), Drainage and imbibition relative permeability relationships for supercritical CO_2/brine and H_2S/brine systems in intergranular sandstone, carbonate, shale, and annhydrite rocks, SPE Reservoir Eval. Eng., 11, 487–496.

Bense, V. F., and M. A. Person (2006) Faults as conduit-barrier systems to fluid flow in siliciclastic sedimentary aquifers, Water Resour. Res., 42, W05421, doi:10.1029/2005WR004480.

Bretan, P., Yielding, G., Mathiassen, O. M., Thorsnes, T. (2011) Fault-seal analysis for CO_2 storage: an example from the Troll area, Norwegian Continental Shelf. Petroleum Geoscience 17: 181-192.

Chang, K., Minkoff, S. E., Bryant, S. L. (2008) Modeling Leakage through Faults of CO_2 Stored in an Aquifer, SPE ATCE, Denver, CO, Sept. 22-25, SPE 115929.

Chang, K., Bryant, S. L. (2009) The Effect of Faults on Dynamics of CO_2 Plumes, Energy Procedia 1:1839-1846.

Chiodini, G. et al. (1999) Quantification of deep CO_2 fluxes from Central Italy. Examples of carbon balance for regional aquifers and of soil diffuse degassing. Chemical Geology. 159:205-222.

Errat, D., Thomas, G. M., et al. (2011) North Sea hydrocarbon systems: some aspects of our evolving insights into a classic hydrocarbon province. Vining, B.A. & PICKERING, S. C. (eds) Petroleum Geology: From Mature Basins to New Frontiers – Proceedings of the 7th Petroleum Geology Conference, 37–56.

Faulkner D. R., C. A. L. Jackson, R. J. Lunn, R. W. Schlische, Z. K. Shipton, C. A. J. Wibberley, M. O. Withjack (2010) A review of recent developments concerning the structure, mechanics and fluid flow properties of fault zones. Journal of Structural Geology 32:1557-1575.

Gammer, D., Green, A., Holloway, S., Smith, G. (2011) The Energy Technologies Institute's UK Storage Appraisal Project (UKSAP). SPE Offshore Europe Oil and Gas Conference and Exhibition held in Aberdeen, UK, 6-8 September 2011. SPE 148426.

Gluyas, J. G., Swarbrick, R. (2004) Petroleum Geoscience. Blackwell Publishing.

Humez, P., Audiagne, P., Lions, J., Chiaberge, C., Bellenfant, G. (2011) Modeling of CO2 Leakage up through an abandoned well from deep saline aquifer to shallow fresh groundwaters. Transport in Porous Media 90:153-181.

LeCain, G. D. (1998) Results from air-injection and tracer testing in the Upper Tiva Canyon, Bow Ridge Fault, and Upper Paintbrush contact alcoves of the exploratory studies facility, August 1994 through July 1996, Yucca Mountain, Nevada, U.S. Geological
Survey, Water-Resources Investigations 98-4058.

Lee, Y., Kim, K., Sung, W., Yoo, I (2010) Analysis of the leakage possibility of injected CO_2 in a saline aquifer, Energy Fuels 24:3292-3298.

Lewicki, J. L., Birkholzer, J., Tsang, C.-F. (2007) Natural and industrial analogues for leakage of CO_2 from storage reservoirs: identification of features, events, and processes and lessons learned. Environmental Geology 52:457-467.

Losh, S., Haney, M., 2006. Episodic fluid flow in an aseismic overpressured growth fault, northern Gulf of Mexico. In: Abercrombie, R., McGarr, A., Di Toro, G., Kanamori, H. (Eds.), Earthquakes: Radiated Energy and the Physics of Faulting. American Geophysical Union Geophysical Monograph Series, vol. 170, pp. 199-206.

Manzocchi, T., J. J. Walsh, P. Nell, and G. Yielding (1999), Fault transmissibility multipliers for flow simulation models, Pet. Geosci. 5:53– 63.

Manzocchi, T., Childs, C., and Walsh, J. J. (2010) Faults and fault properties in hydrocarbon flow models: Geofluids, 10:94–113, doi:10.1111/j.1468-8123.2010.00283.x.

Mathias, S. A., Hardisty, P. E., Trudell, M. R., Zimmerman, R. W. (2009) Screening and selection of sites for CO_2 sequestration based on pressure buildup. International Journal of Greenhouse Gas Control 3(5): 577-585.

Mathias, S. A., Gluyas, J. G., Gonzalez, G., Hosseini, S. (2011) Role of partial miscibility on pressure buildup due to constant rate injection of CO_2 into closed and open brine aquifers. Water Resources Research 47: W12525.

Miller, S. A., Collettini, C., Chiaraluce, L., Cocco, M., Barchi, M., Kaus, B. J. P. (2004) Aftershocks driven by a high-pressure CO_2 source at depth. Nature 427 (6976), 724-727.

Myers R. D., Allgood A., Hjellbakk A., Vrolijk P., Briedis N. (2007) Testing fault transmissibility prediction in a structurally dominated reservoir: Ringhorne field, Norway. In: Structurally Complex Reservoirs (eds Jolley SJ, Barr D, Walsh JJ, Knipe RJ), Geological Society of London Special Publication, 292, 271–94.

Noir, J., Jacques, E., Bekri, S., Adler, P. M., Tapponnier, P., King, G.C.P., 1997. Fluid flow triggered migration of events in the 1989 Dobi earthquake sequence of Central Afar. Geophysical Research Letters 24 (18), 2335e2338.

O'Brien, G. W., Woods, E. P. (1995) Hydrogen-related diagenetic zones (HRDZs) in the Vulcan sub-basin, Timor Sea: Recognition and exploration implications. APEA Journal 220-237.

Pearce, J. et al. (2002) Natural CO_2 accumulations in Europe: Understanding long-term geological processes in CO_2 sequestration. Proceedings of the 6th International Conference on Greenhouse Gas Control Technologies GHGT-6. Vancouver, Canada. 105-111.

Pruess, K. (2005) Numerical studies of fluid leakage from a geologic disposal reservoir for CO_2 show self-limiting feedback between fluid flow and heat transfer. Geophys. Res. Lett. 32 (14), L14404, doi:10.1029/2005GL023250.

Pruess K., Nordbotten J. (2011) Numerical simulation studies of the long-term evolution of a CO_2 plume in a saline aquifer with a sloping caprock. Transport in Porous Media doi: 10.1007/s11242-011-9729-6

Pruess, K. (2011) Integrated modeling of CO_2 storage and leakage scenarios including transitions between super- and subcritical conditions, and phase change between liquid and gaseous CO_2. Greenhouse Gas Sci Technol. 1:237–247.

Sarginson, M. J. (2003) The Barque Field, Blocks 48/13a, 48/14, UK North Sea. Geological Society, London, Memoirs January 1, 2003, v. 20, p. 661-670.

Streit, J., Hillis, R. (2004) Estimating fault stability and sustainable fluid pressures for underground storage of CO_2 in porous rock. Energy 29:1445–1456.

Streit, J. M., Watson, M. N. (2004) Estimating rates of potential CO_2 loss from geological storage sites for risk and uncertainty analysis. Proceedings of the 7th International Conference on Greenhouse Gas Control Technologies GHGT-7. Vancouver, Canada. 1309-1314.

Talwani, P., L. Chen, and K. Gahalaut (2007), Seismogenic permeability, ks, J. Geophys. Res., 112, B07309, doi:10.1029/2006JB004665.

Tueckmantel, C., Fisher, Q. J., Manzocchi, T., Skachkov, S., Grattoni, C. A. (2012) Two-phase fluid flow properties of cataclastic fault rocks: Implications for CO_2 storage in saline aquifers. Geology 40:39-42.

Underschultz, J. (2007) Hydrodynamics and membrane seal capacity. Geofluids. 7:148-158.

van der Zee, W., Urai, J. L. (2005) Processes of normal fault evolution in a siliciclastic sequence: a case study from Miri, Sarawak, Malaysia. Journal of Structural Geology 27: 2281-2300.

Van Hulten, F. F. N. (2010) Geological factors effecting compartmentalization of Rotliegend gas field in the Netherlands. Jolley, S. J., Fisher, Q. J., Ainsworth, R. B., Vrolijk, P. J. & Delisle, S. (eds) Reservoir Compartmentalization. Geological Society, London, Special Publications, 347, 301–315.

Wibberley, C. A. J., Yielding, G., Di Toro, G. (2008) Recent advances in the understanding of fault zone internal structure; a review. In: Wibberley, C. A. J., Kurz, W., Imber, J., Holdsworth, R. E., Collettini, C. (Eds.), Structure of Fault Zones: Implications for Mechanical and Fluid-flow Properties. Geological Society of London Special Publication, vol. 299, pp. 5-33.

Wilins, S. J., Naruk, S. J. (2007) Quantitative analysis of slip-induced dilation with application to fault seal. AAPG Bulletin 91: 97-113.

Wiprut D., Zoback M. D. (2000) Fault reactivation and fluid flow along a previously dormant normal fault in the northern North Sea. Geology, 28, 595–8.

Zhang, Y., Oldenburg, C. M., Finsterle, S. (2010) Percolation-theory and fuzzy rule-based probability estimation of fault leakage at geologic carbon sequestration sites. Environ. Earth Sci. 59:1447–1459.

8.0 Tables and figures

Table 1: Summary of CO_2 fault leakage natural analogues from Lewicki et al. (2007).

Site	CO_2 source and geologic model for accumulation	Event triggering leakage and type of surface leakage	Magnitude of surface CO_2 or CH_4 leakage
A1. Mammoth Mountain, CA USA	Magmatic + thermal decomposition of carbonates. Accumulation at 2 km depth in porous/fractured rock under caprock.	Seismic activity and reservoir pressurization. Fast, diffuse, vent, spring.	~ 250 t day^{-1} from 480,000 m^2 area
A2. Solfatara, Italy	Magmatic + thermal decomposition of carbonates. Relatively shallow zone of fractured rock contains gas phase and overlies aquifers, then magma body at several km depth.	No specific leakage event captured. Diffuse and vent.	1,500 t day^{-1} from 0.5 km^2 area
A3. Albani Hills, Italy	Magmatic + thermal decomposition of carbonates. Deep pressurized reservoirs in structural highs of sedimentary bedrock.	Slow releases with several sudden large releases also occurring, possibly triggered by seismic activity. Diffuse, vent, spring/well, 1995 and 1999 events fast.	74 t day^{-1} as surface gas emissions (61,000 m^2 area) and 506 t day^{-1} as dissolved CO_2 in shallow ground water
A4. Clear Lake, CA, USA	Thermal decomposition of metasedimentary rocks, minor magmatic component. CO2 derived from liquid-dominated geothermal reservoir hosted in marine metasedimentary rocks.	No specific leakage event captured. Gas vents, springs.	~ 1 t day^{-1}
A6. Mátraderecske, Hungary	Geothermal/copper-zinc mineralization. CO2 accumulates in karst water reservoir (1 km depth).	No specific leakage event captured. Diffuse, vent, spring.	Average CO_2 flux 200–400 g m^{-2} day^{-1} (total degassing area unknown)
A12. Paradox Basin, UT, USA	Thermal decomposition of carbonates. Reservoirs are vertically stacked, sandstone units, in fault-bounded anticlinal folds, capped by shale/siltstone units.	No specific leakage event captured. Diffuse, gas seeps, springs.	Soil CO_2 fluxes up to 100 g $m^{-2}day^{-1}$; total emission rate unknown

Site	Leakage pathway	CO_2 leakage rate (t / yr /m^2)	Reference
A1. Mammoth Mountain, CA USA	Faults and fractures	0.19	Lewicki et al. (2007)
A2. Solfatara, Italy	Faults and fractures	1.10	Lewicki et al. (2007)
A3. Albani Hills, Italy	Faults and fractures	0.44	Lewicki et al. (2007)
A12. Paradox Basin, UT, USA	Faults and fractures	0.04	Lewicki et al. (2007)
Otway (Penola)	Fault conduit	5.70E-03	Streit and Watson (2004)
Otway (Pine Lodge)	Fault conduit	1.50E-02	Streit and Watson (2004)
Otway (Pine Lodge)	Permeable zone	3.7E-03 to 7.5E-03	Streit and Watson (2004)
Mátraderecske, Hungary	Fault conduit	< 6.4	Pearce et al. (2002)
Latera, Tuscany	Permeable zone	39.4	Pearce et al. (2002)
Mesozoic carbonate	Permeable zone	1.76E-5 to 3.96E-4	Chiodini et al. (1999)
Numerical simulation	Fault conduit	2208 to 2522	Chang et al. (2008)
Numerical simulation	Fault conduit	12.61	Pruess (2011)

Table 2: Summary of natural analogues and numerically simulated surface leakage rates.

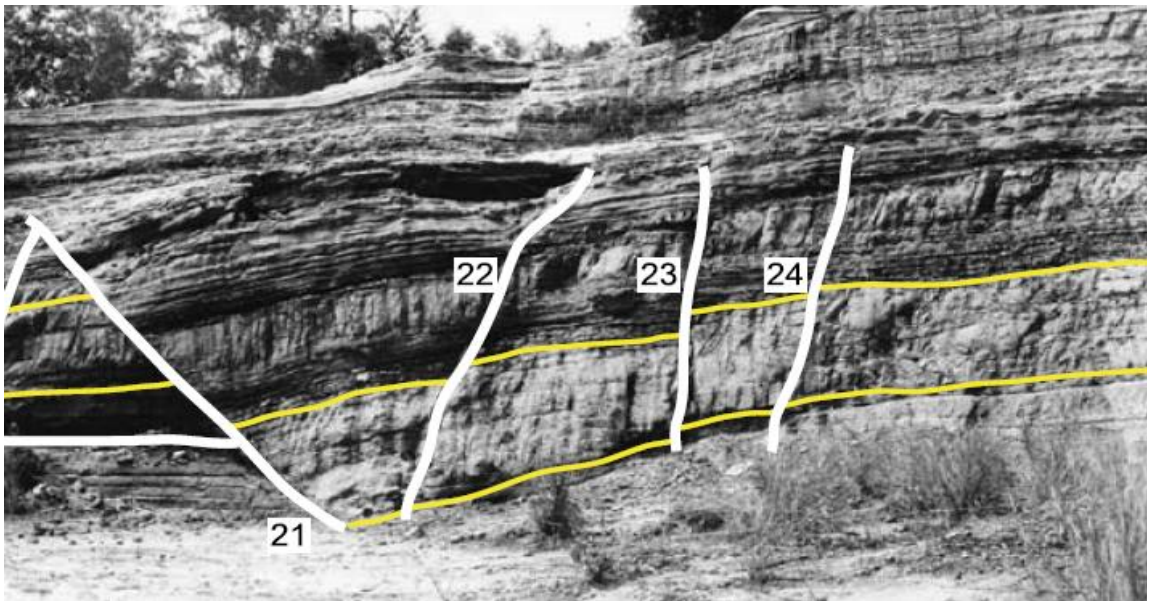

Fig. 1: A faulted deltaic sand–clay sequence near Miri, Sarawak (van der Zee and Urai, 2005).

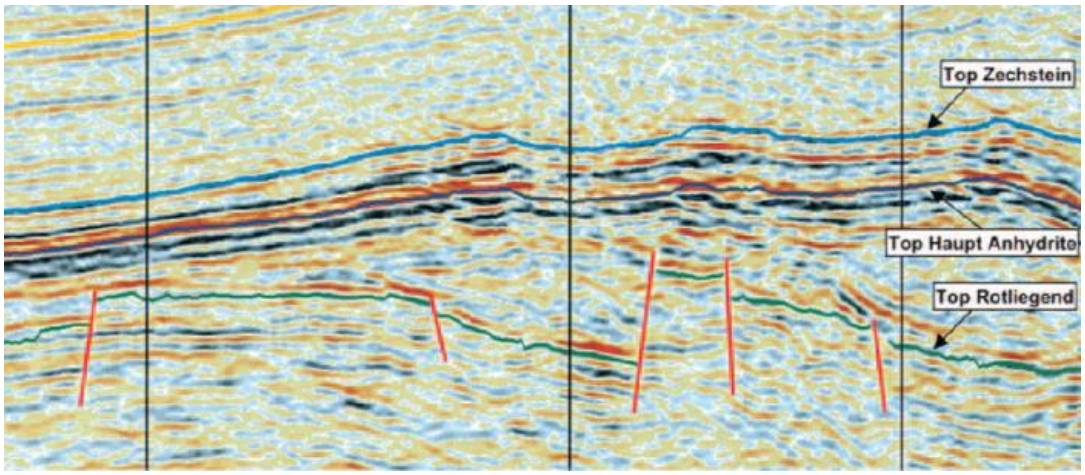

Fig. 2: Seismic section showing faulting in the Rotliegend sandstone (Sarginson, 2003).

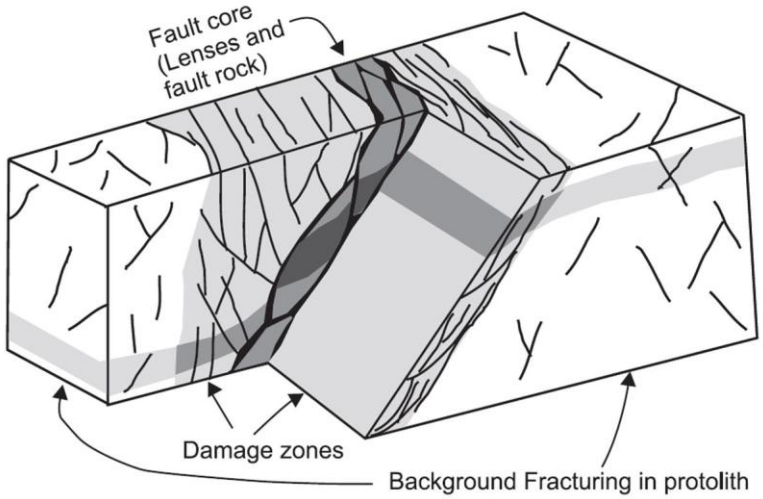

Fig. 3: Schematic of damage zone and core structure (Manzocchi et al., 2010).

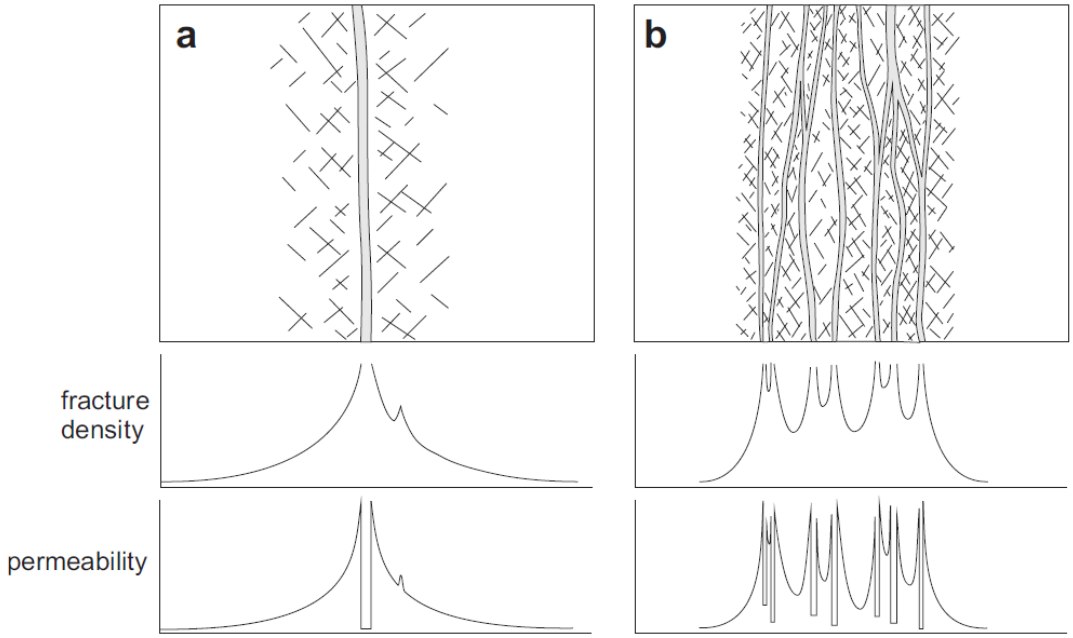

Fig. 4: Schematic showing permeability distribution in damage zone and core fault structures a) for a single fault and b) a fault zone containing multiple cores (Faulkner et al., 2010).

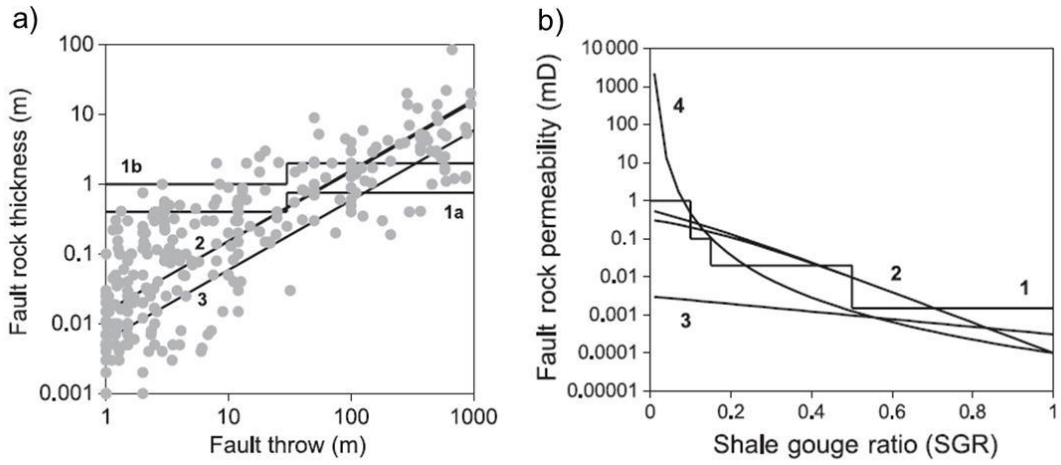

Fig. 5: Fault properties for production simulation (Manzocchi et al., 2010). a) Fault rock thickness relationships used in successful history-matched flow simulation models. The dots are individual fault rock thickness measurements from outcrop. b) Fault permeability used in successful history-matched flow simulation models.

Fig 6: The clay beds are sheared into the fault zone, and coalesce into a thick clay gouge. The sand beds are disrupted, but are not incorporated into the gouge. (from van der Zee and Urai, 2005)

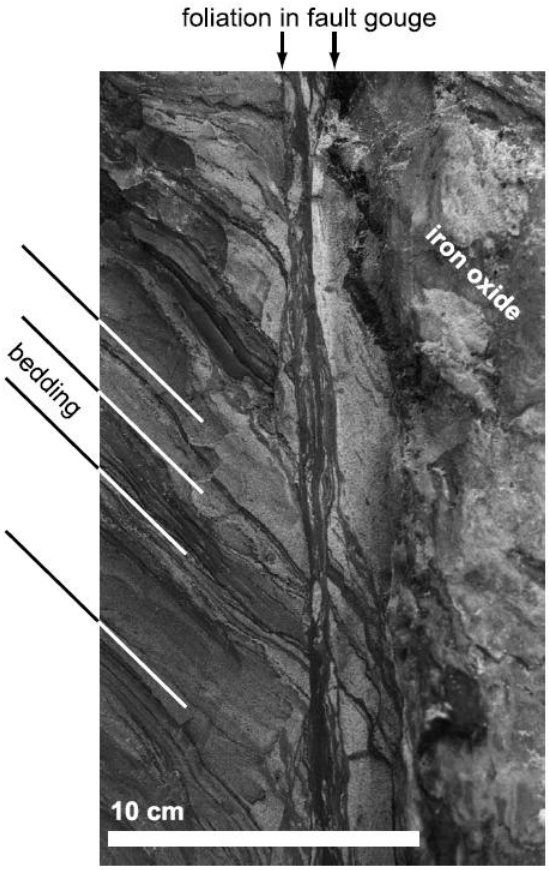

Fig. 7: The sheared sand and clay in the fault develop into a foliated gouge. On the right side of the fault zone there is a hard oxide layer, which presumably formed as a weathering product from

groundwater flowing downwards along the right side of this sealing fault. (from van der Zee and Urai, 2005)

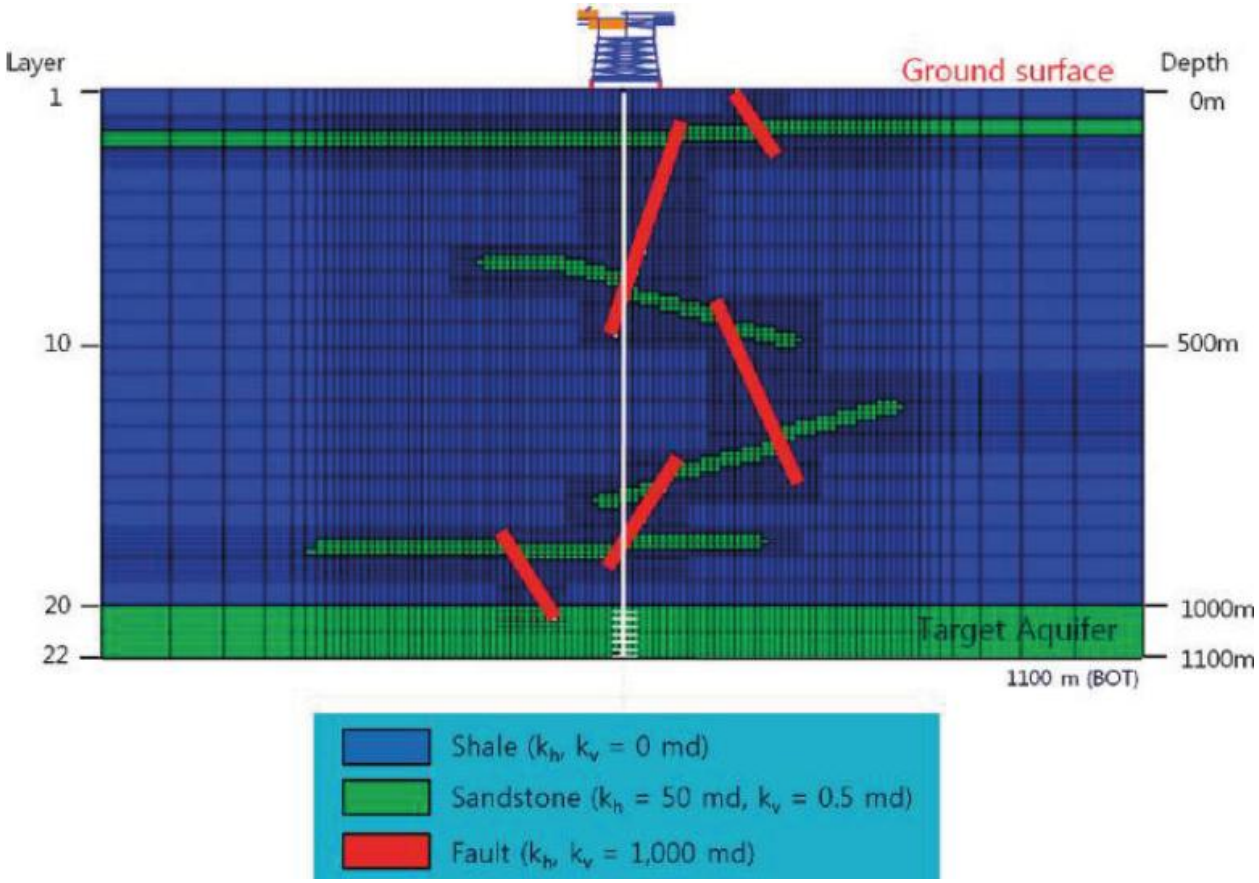

Fig. 8: Schematic of model setup used by Lee et al. (2010) to look at the role of fault connectivity on CO_2 leakage.

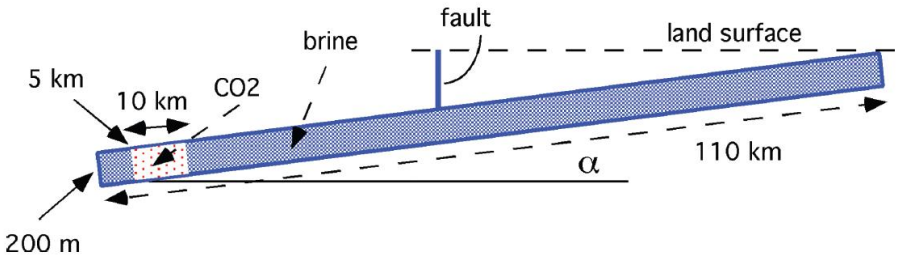

Fig. 9: Schematic of model setup used by Pruess (2011) to look at migration of a CO_2 plume in a sloping aquifer, intersected by a fault. The assumed initial CO_2 plume is shown by light shading.

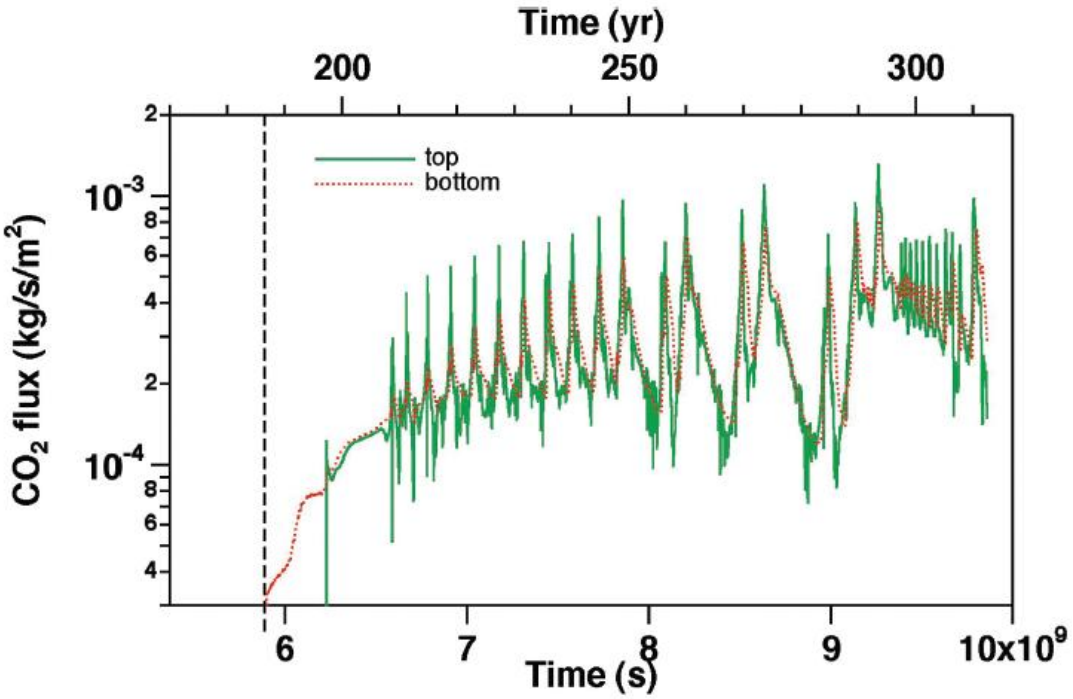

Fig. 10: Simulated CO_2 fluxes at the top and bottom of the fault (after Pruess, 2011).

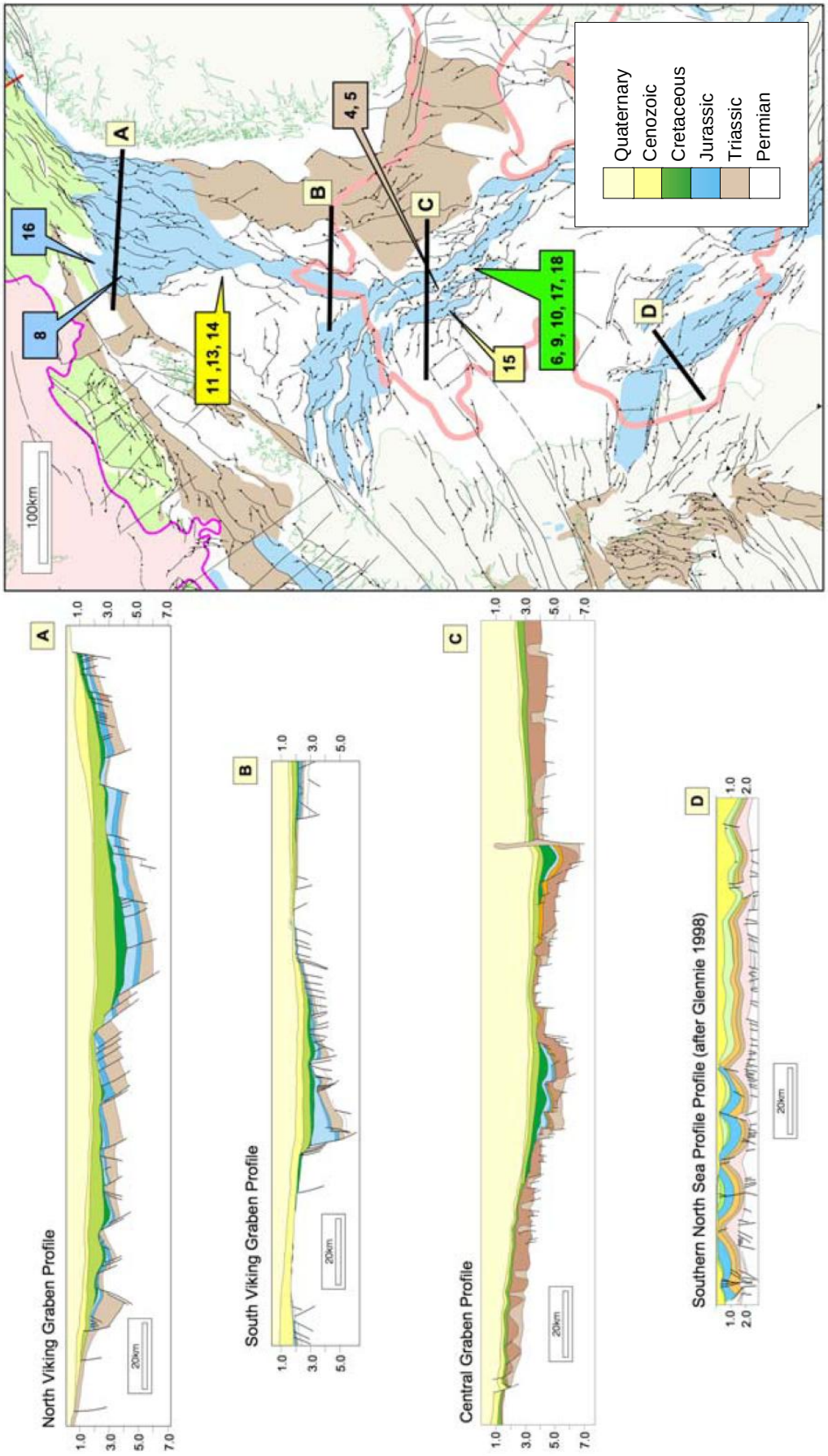

Fig. 11: A series of sections and a map showing structural elements of the North Sea Rift. Map shows principal fault trends at the Base Cretaceous. Colour scheme on map shows timing of principal rift events as shown in key (Cenozoic, Cretaceous, etc.). (after Erratt et al., 2011).